

Supplementary Information

Enhancing the Activity and Stability of Carbon-Supported Platinum-Gadolinium Nanoalloys towards the Oxygen Reduction Reaction

Carlos A. Campos-Roldán^a, F. Pailloux^b, P.-Y. Blanchard^a, D. J. Jones^a, J. Rozière^a,
S. Cavaliere^{a,c*}

^a ICGM, Université de Montpellier, CNRS, ENSCM, 34095 Montpellier cedex 5, France

^b Institut P', CNRS - Université de Poitiers – ISAE-ENSMA - UPR 3346, 11 Boulevard Marie
et Pierre Curie, Site du Futuroscope, TSA 41123, 86073 Poitiers cedex 9, France

^c Institut Universitaire de France (IUF), 1 rue Descartes

75231 Paris cedex 05, France

Corresponding author: Sara.Cavaliere@umontpellier.fr

S1. Experimental details

Synthesis of carbon supported Pt_xGd nanoalloys

From our previous study,¹ the optimal Pt:Gd composition has been identified. Based on this conclusion, we have synthesized the Pt_xGd/C following the protocol proposed by Hu et al.² with minimal modifications: 0.45 g of commercial carbon Vulcan XC-72 (Cabot), 2 g of CN₂H₂ (< 99%, Sigma-Aldrich), 0.358 g of GdCl₃ (anhydrous powder, 99.99% from Sigma-Aldrich) and 0.5 g of H₂PtCl₆·6H₂O (Sigma-Aldrich) were blended in an agate mortar at room conditions, forming a thick slurry. The resulting slurry was transferred into a tubular furnace, which was purged with 4%H₂/N₂ and heated up to 180 °C at 10 °C min⁻¹ for 30 min. Then, the temperature was raised to 650 °C at 10 °C min⁻¹ for 120 min. After that, the furnace was cooled down naturally until room temperature, obtaining the as-prepared material.

Acid wash under air atmosphere

0.5 g of the as-prepared material were added in 500 mL of 0.5 M H₂SO₄. The temperature of the suspension was held at 70 °C for 60 min under air atmosphere and magnetically stirred. Thereafter, the catalyst was filtered at vacuum, thoroughly washed with Mili-Q water and vacuum-dried at 80 °C overnight.

Acid leaching under N₂ atmosphere

500 mL of 0.5 M H₂SO₄ were saturated with N₂ for 1 h. Then, 0.5 g of the as-prepared material were added and magnetically stirring for 4 h holding the N₂ atmosphere.

Thereafter, the catalyst was filtered at vacuum, thoroughly washed with Mili-Q water and vacuum-dried at 80 °C overnight.

Inductively Coupled Plasma Mass Spectrometry (ICP-MS): An Agilent 7800 ICP-MS equipped with a Micromist/Scott nebulizer was used. The sample mineralization was carried out in an Anton-Paar Multiwave Pro with 600 W for 40 min.

X-Ray diffraction (XRD): The XRD patterns were recorded in a Panalytical X'Pert Pro diffractometer, equipped with a Cu K α radiation source ($\lambda=1.541 \text{ \AA}$), using a scan rate of 0.5 ° min $^{-1}$, in the range $10^\circ \leq 2\theta \leq 90^\circ$.

Transmission Electron Microscopy (TEM, STEM): A small portion of each sample was dispersed in isopropanol for 30 min, and an aliquot was deposited on a lacey-carbon film supported by on a copper grid and dried at room temperature. The bright-field TEM micrographs were acquired in a JEOL 1200 EXII microscope operating at 120 kV, equipped with a CCD camera SIS Olympus Quemesa. The HAADF-STEM study was carried out in a JEOL-2200FS microscope operated at 200 kV (Schottky-FEG emitter) and fitted with an in-column omega-filter and a GATAN Ultrascan CCD 2048x2048 px 2 camera, using the same conditions respect to our previous study.¹

X-Ray Photoelectron Spectroscopy (XPS): The near-surface analysis was carried out in an X-ray photoelectron spectrometer ESCALAB 250 (Thermo Electron) with a monochromatic Al

K α X-ray source (1486.6 eV), analyzing 400 μm^2 of the sample. Survey and high-resolution spectra were acquired using analyzer pass energies of 160 and 20 eV, respectively. The binding energy of C=C (284.6 eV) was used as internal calibration energy. Data analysis was carried out using the Avantage software. Before fitting, a Shirley background was subtracted from raw data. For the core level 4f Pt photoemission lines, the doublet separation was set to 3.33 eV, and the ratio between the components was set to 1.33. The core level 4d Gd spectra, however, is in general a complex broad multiplet structure, due to the presence of localized electrons in the 4f shell and spin-orbit coupling.³ Therefore, we carried out a comparison with the reference spectrum of a sputter-cleaned Pt₅Gd polycrystalline alloy reported by Velazquez-Palenzuela et al.,³ from where the Gd atoms are in completely metallic state.

Electrochemical measurements: A Pt loading (L_{Pt}) of 20 $\mu\text{g}_{\text{Pt}} \text{cm}^{-2}_{\text{geo}}$ was achieved by ultrasonically ca. 3.5 mg of the catalyst powder in 1 mL of isopropanol, 12 μL of Nafion[®] 5% v/v and 3.988 mL of Mili-Q water, and carefully deposit 20 μL of the resulting suspension onto a glassy carbon electrode (0.196 cm^2). The deposited ink was dried at room conditions by rotating the electrode at 450 rpm.

A standard three-electrode glass cell was used, where a reversible hydrogen electrode (RHE) and a graphite rod isolated in a glass-fritted compartment served as reference and counter electrode, respectively. All measurements were performed at 20 \pm 1 $^{\circ}\text{C}$.

Cyclic voltammetry (CV) was carried out from 0.050 to 0.925 V in N₂-saturated 0.1 M HClO₄. The electrochemical active surface area (ECSA) was calculated from the CO-stripping method at 20 mV s⁻¹. The ORR polarization curves were recorded by linear sweep voltammetry, from 0.05 to 1.05 V at 20 mV s⁻¹, in O₂-saturated 0.1 M HClO₄. The ohmic drop was determined by electrochemical impedance spectroscopy (EIS). The accelerated stress test (AST) was performed applying 10000 cycles using a triangle-shape wave (0.600-0.925 V) at 100 mV s⁻¹ in N₂-saturated 0.1 M HClO₄. The ECSA and ORR polarization curves were measured before and after the AST. For comparative purposes, 40% wt. Pt/C from Johnson-Matthey was used as benchmark.

S2. Powder XRD patterns

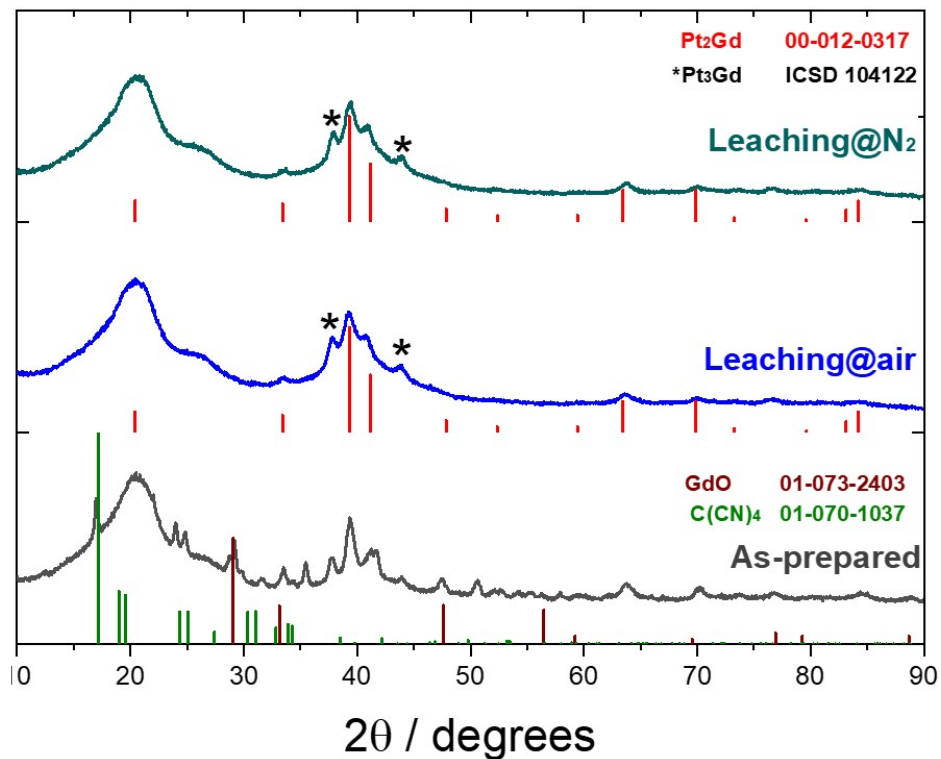


Figure S1. Powder XRD patterns of the as-prepared Pt_xGd/C, and air- or N₂-leaching Pt_xGd/C.

In all cases, the Pt-Gd alloy is confirmed. The as-prepared electrocatalysts present reflections attributed to cyanamide complexes and rare earth oxides. Regardless the atmosphere, these reflections do not appear after the acid leaching treatment, confirming the removal of such undesirable reaction residues.

S3. Electron microscopy

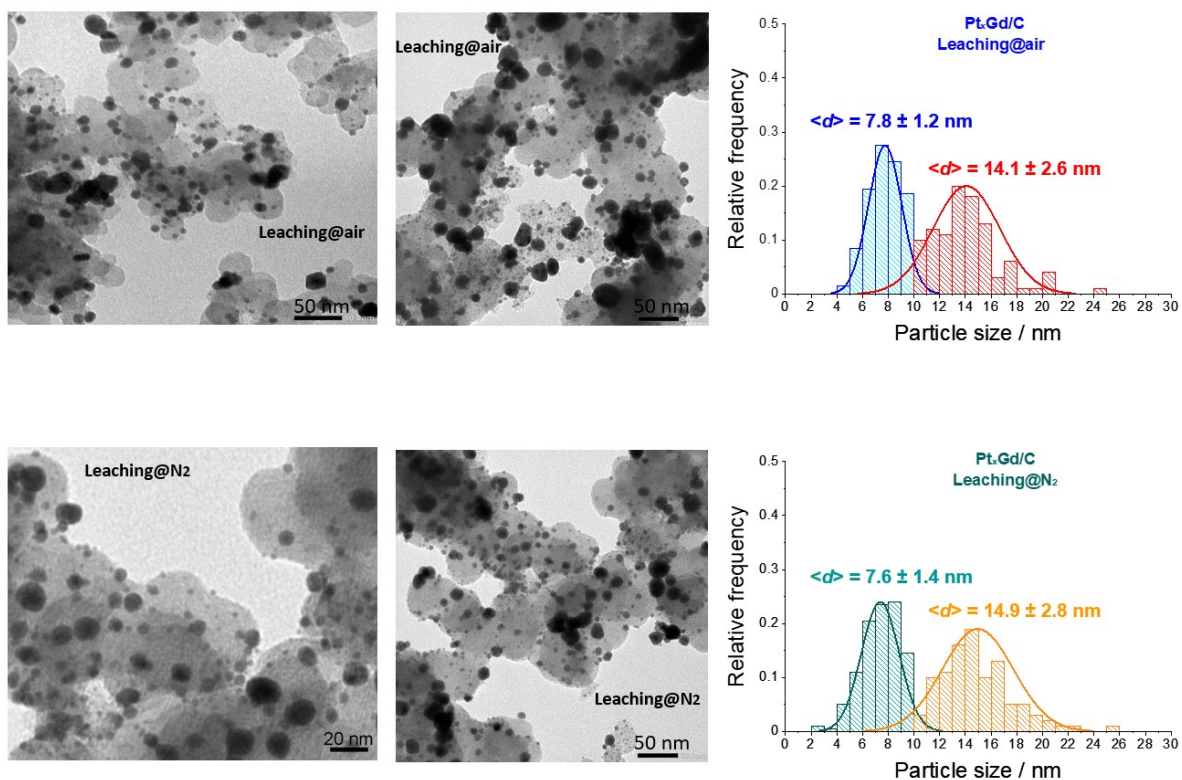


Figure S2. TEM micrographs and particle size distribution of air- or N₂-leaching Pt_xGd/C.

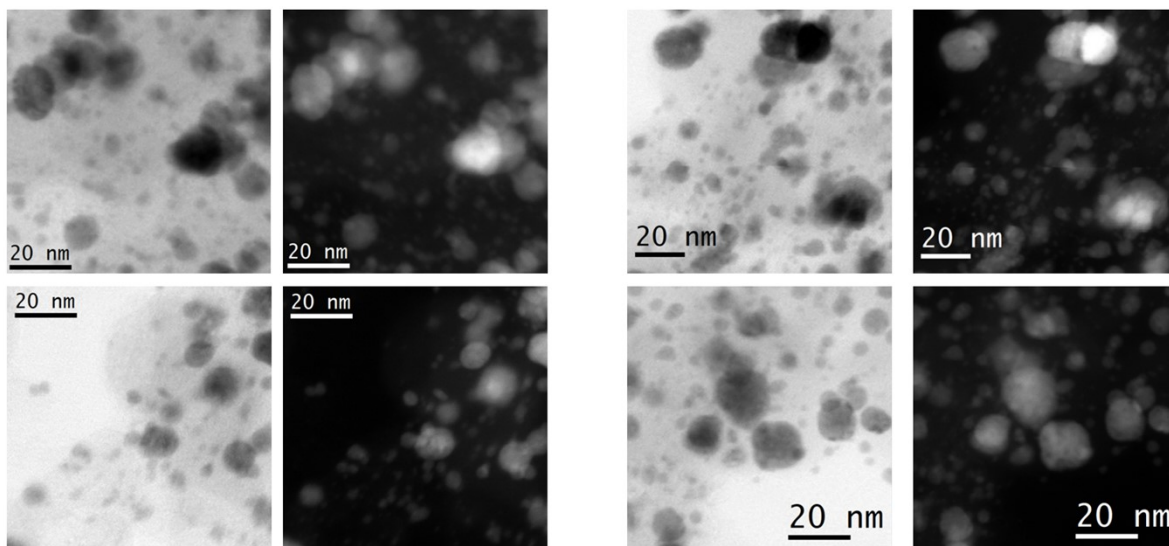


Figure S3. Complementary STEM micrographs of N₂-leaching Pt_xGd/C.

S4. Surface electrochemistry

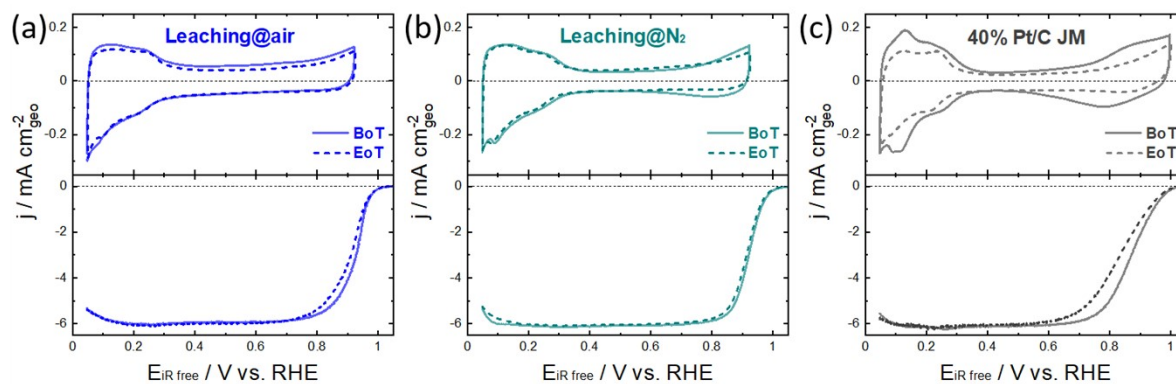


Figure S4. Cyclic voltammograms (N₂-saturated 0.1 M HClO₄ at 20 mV s⁻¹) and ORR polarization curves (O₂-saturated 0.1 M HClO₄ at 20 mV s⁻¹ and 1600 rpm) at BoT and EoT of (a) Pt/Gd/C leaching@air, (b) Pt/Gd/C leaching@N₂, and (c) 40% wt. Pt/C JM.

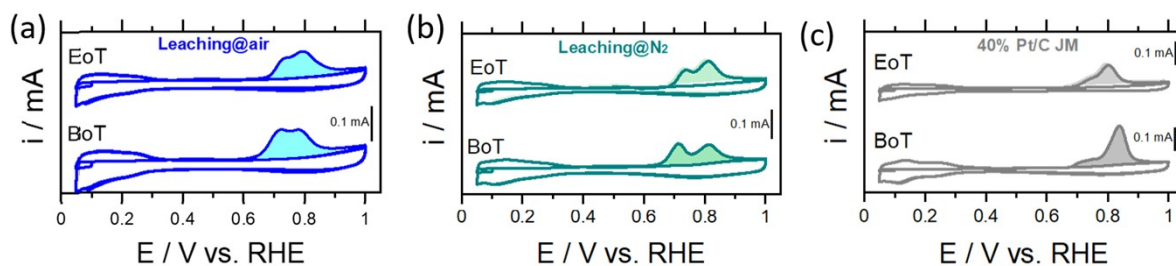


Figure S5. CO-stripping profiles, at 20 mV s⁻¹ and at BoT and EoT of (a) Pt/Gd/C leaching@air, (b) Pt/Gd/C leaching@N₂, and (c) 40% wt. Pt/C JM.

ECSA determination

The electrochemically active surface area (ECSA) was calculated from the CO-stripping method at 20 mV s⁻¹ as previously suggested for Pt-REM alloys.⁴ After the surface activation, the electrode potential was held at 0.1 V vs. RHE and CO was bubbling for 5 min. After that, the gas was switch back to N₂ for 20 min to remove the residual CO in the solution. Then, three potential cycles were performed between 0.05-1.0 V.

Next, the second cycle of the experiment was used as background and was subtracted from the first cycle. The CO oxidation charge was calculated by the integration of the background-corrected curve from 0.4-1.0 V and its correction for the scan rate⁵:

$$Q = \frac{1}{\nu} \int_{0.4}^{1.0} i \, dE \quad [=] \, \mu C \quad (1)$$

The platinum surface (S_{Pt}) was calculated assuming a theoretical value of $Q_0 = 420 \, \mu C \, cm_{Pt}^{-2}$ for the electro-oxidation of an adsorbed CO monolayer:

$$S_{Pt} = \frac{Q}{Q_0} [=] \, cm_{Pt}^{-2} \quad (2)$$

Finally, the ECSA was derived from the normalization of S_{Pt} respect to the Pt loading (L_{Pt}):

$$ECSA = \frac{S_{Pt}}{L_{Pt} \cdot A_{geo}} \cdot \left| \frac{10^6 \, \mu g_{Pt}}{g_{Pt}} \cdot \frac{m_{Pt}^2}{10^4 \, cm_{Pt}^2} \right| [=] \, m_{Pt}^2 \, g_{Pt}^{-1} \quad (3)$$

Where $L_{Pt} = 20 \, \mu g_{Pt} \, cm_{geo}^{-2}$; $A_{geo} = 0.196 \, cm_{geo}^2$.

ORR activity determination

The ORR polarization curves were recorded by linear sweep voltammetry, from 0.05 to 1.05 V vs. RHE at 20 mV s⁻¹ at 1600 rpm. The ohmic drop was determined by electrochemical impedance spectroscopy (EIS) and corrected before experiment by the potentiostat:

$$E_{corr} = E - iR \quad [=] \, V \quad (4)$$

The background scan was recorded in N₂-saturated 0.1 M HClO₄. Thereafter, the solution was saturated with O₂ and the polarization curves were carried out under the same conditions. Then, the background scan was subtracted from the ORR polarization curve and normalized by geometric area (c.f. Figure S9):

$$j = \frac{i_{O_2} - i_{N_2}}{A_{geo}} [=] mA cm_{geo}^{-2} \quad (5)$$

For practical purposes, the calculation was performed using the ORR current, $i_T = i_{O_2} - i_{N_2}$, rather than the ORR current density, j , (i.e. no normalization by the geometric area).

The diffusion limiting current, i_d , was obtained at the potential range where the reaction is governed by the mass-transport process (i.e. 0.4 V vs. RHE). After that, the kinetic current, i_k , was calculated through the Koutecky-Levich equation:

$$i_k = \frac{i_{dif} \cdot i_T}{i_{dif} - i_T} [=] mA \quad (6)$$

The ORR specific activity, I_s , was calculated from the normalization of i_k respect to the Pt surface S_{Pt} :

$$I_s = \frac{i_k}{S_{Pt}} [=] mA cm_{Pt}^{-2} \quad (7)$$

and the ORR mass activity, I_m , was calculated from the normalization of i_k respect to the Pt loading L_{Pt} :

$$I_m = \frac{i_k}{L_{Pt} \cdot A_{geo}} \cdot \left| \frac{A}{10^3 mA} \cdot \frac{10^3 \mu g_{Pt}}{mg_{Pt}} \right| [=] A mg_{Pt}^{-1} \quad (8)$$

REFERENCES

1. C.A. Campos-Roldán, F. Pailloux, P. Blanchard, D. Jones, J. Roziere, S. Cavaliere, *Submitted for publication* **2021**.
2. Hu, Y.; Jensen, J. O.; Cleemann, L. N.; Brandes, B. A.; Li, Q., Synthesis of Pt-Rare Earth Metal Nanoalloys. *J Am Chem Soc* **2020**, *142* (2), 953-961.
3. Velázquez-Palenzuela, A.; Masini, F.; Pedersen, A. F.; Escudero-Escribano, M.; Deiana, D.; Malacrida, P.; Hansen, T. W.; Friebel, D.; Nilsson, A.; Stephens, I. E. L.; Chorkendorff, I., The enhanced activity of mass-selected Pt_xGd nanoparticles for oxygen electroreduction. *J. Catal.* **2015**, *328*, 297-307.
4. Escudero-Escribano, M.; Jensen, K. D.; Jensen, A. W., Recent advances in bimetallic electrocatalysts for oxygen reduction: design principles, structure-function relations and active phase elucidation. *Curr Opin Electrochem* **2018**, *8*, 135-146.
5. Mayrhofer, K. J. J.; Strmcnik, D.; Blizanac, B. B.; Stamenkovic, V.; Arenz, M.; Markovic, N. M., Measurement of oxygen reduction activities via the rotating disc electrode

method: From Pt model surfaces to carbon-supported high surface area catalysts. *Electrochim Acta* **2008**, 53 (7), 3181-3188.